Water Resources Research

RESEARCH ARTICLE
10.1029/2020WR027772

On the Limitations and Implications of Modeling Heat Transport in Porous Aquifers by Assuming Local Thermal Equilibrium

Manuel A. Gossler[1], Peter Bayer[2], Gabriel C. Rau[3,4], Florian Einsiedl[1], and Kai Zosseder[1]

[1]Chair of Hydrogeology | Department of Civil, Geo and Environmental Engineering, Technical University of Munich, Munich, Germany, [2]Department of Applied Geosciences, Martin Luther University of Halle-Wittenberg, Halle/Saale, Germany, [3]Institute of Applied Geosciences, Karlsruhe Institute of Technology (KIT), Karlsruhe, Germany, [4]School of Civil and Environmental Engineering, UNSW, Sydney, Australia

Key Points:
- Local thermal nonequilibrium effects can occur in porous aquifers in high-velocity zones with large grain sizes or near pumping wells
- Thermal dispersion can be increased up to a factor of over 30 by local thermal nonequilibrium effects
- Advective thermal velocity is not significantly influenced by local thermal nonequilibrium effects for most simulations (95%)

Supporting Information:
- Supporting Information S1

Correspondence to:
M. A. Gossler and K. Zosseder,
manuel.gossler@tum.de;
kai.zosseder@tum.de

Citation:
Gossler, M. A., Bayer, P., Rau, G. C., Einsiedl, F., & Zosseder, K. (2020). On the limitations and implications of modeling heat transport in porous aquifers by assuming local thermal equilibrium. *Water Resources Research*, *56*, e2020WR027772. https://doi.org/10.1029/2020WR027772

Received 22 APR 2020
Accepted 21 SEP 2020
Accepted article online 25 SEP 2020

Abstract Heat transport in natural porous media, such as aquifers or streambeds, is generally modeled assuming local thermal equilibrium (LTE) between the fluid and solid phases. Yet, the mathematical and hydrogeological conditions and implications of this simplification have not been fully established for natural porous media. To quantify the occurrence and effects of local thermal disequilibrium during heat transport, we systematically compared thermal breakthrough curves from a LTE with those calculated using a local thermal nonequilibrium (LTNE) model, explicitly allowing for different temperatures in the fluid and solid phases. For the LTNE model, we developed a new correlation for the heat transfer coefficient representative of the conditions in natural porous aquifers using six published experimental results. By conducting an extensive parameter study (>50,000 simulations), we show that LTNE effects do not occur for grain sizes smaller than 7 mm or for groundwater flow velocities that are slower than 1.6 m day^{-1}. The limits of LTE are likely exceeded in gravel aquifers or in the vicinity of pumped bores. For such aquifers, the use of a LTE model can lead to an underestimation of the effective thermal dispersion by a factor of up to 30 or higher, while the advective thermal velocity remains unaffected for most conditions. Based on a regression analysis of the simulation results, we provide a criterion which can be used to determine if LTNE effects are expected for particular conditions.

1. Introduction

Understanding advective heat transport in porous aquifers is of high interest in various areas. For example, reliable prediction of thermal plumes in shallow geothermal energy systems is crucial for a sustainable operation, especially in densely used aquifers (Böttcher et al., 2019; Ferguson, 2009; Hähnlein et al., 2013; Pophillat et al., 2020). Furthermore, heat serves as a valuable tracer to quantify surface water-groundwater interactions (Halloran et al., 2016; Irvine et al., 2020; Irvine & Lautz, 2015; Kurylyk et al., 2019; Rau et al., 2010, 2012b, 2017), to estimate mean water transit times (Bakker et al., 2015; Bekele et al., 2014), and to infer hydraulic conductivity fields (Seibert et al., 2014; Somogyvári & Bayer, 2017; Somogyvári et al., 2016).

Generally, local thermal equilibrium (LTE) is assumed when modeling heat transport. LTE is defined as an instant exchange of thermal energy between the solid and the fluid phases of a porous medium, an assumption which neglects potential temperature differences (Quintard et al., 1997). The LTE assumption allows for merging of the two separate energy equations describing temperature in the fluid and solid phases into one, simplifying the modeling procedure by volumetric averaging (Whitaker, 1991). Previous work about the validity of the LTE assumption in porous media focused on engineering applications such as packed bed reactors (Al-Nimr & Abu-Hijleh, 2002; Al-Sumaily et al., 2013; Amiri & Vafai, 1998; Khashan & Al-Nimr, 2005). While several criteria exist to examine the appropriateness of the LTE assumption for such applications (Amiri & Vafai, 1998; Hamidi et al., 2019; Kim & Jang, 2002; Minkowycz et al., 1999; Zanoni et al., 2017; Zhang et al., 2009), a thorough investigation of the conditions under which LTE is valid for flow in porous aquifers is currently lacking. In fact, adopting the criteria developed for engineering purposes is not straightforward, as the experimental conditions and reference parameters are not representative for

those typical of flow in porous aquifers. For example, the required "characteristic length" in technical applications is commonly defined as channel length or width and cannot easily be determined for heat transport in subsurface environments.

Some of the few studies focusing on geotechnical applications showed that the LTE assumption can fail in geothermal systems hosted in fractured rocks (Heinze et al., 2017; Heinze & Hamidi, 2017; Shaik et al., 2011), in partly saturated systems, for example, during infiltration of rain or melt water in frozen soil (Heinze & Blöcher, 2019), in fractured rocks as heterogeneous porous media with large permeability contrasts (Hamidi et al., 2019), and under streambed conditions with very low Reynolds numbers (Roshan et al., 2014). In these cases, a local thermal nonequilibrium (LTNE) model may be applied. LTNE models apply two separate energy equations to describe the temperature in the fluid and solid phases (Sözen & Vafai, 1990) that are coupled through a heat transfer term which is dependent on the heat transfer coefficient and the heat transfer area. The heat transfer coefficient is a fundamental physical parameter whose value is determined experimentally (Kaviany, 1995). Again, available experimental work stems from the engineering field, and the derived parameter values and correlations are valid only under certain conditions (Singhal et al., 2017a, 2017b; Sun et al., 2015; Tavassoli et al., 2013, 2015; Zhu et al., 2019). For instance, these correlations are mostly derived from air or gas as the fluid, using high Reynolds numbers and wider porosity ranges that are commonly found in porous aquifers (Gunn, 1978; Tavassoli et al., 2015; Zhu et al., 2019). In addition, most of these models assume perfect spheres with a single size (Sun et al., 2015) that cannot be assumed for a heterogeneous and anisotropic aquifer. Furthermore, it is difficult to identify and quantify the errors induced by using an LTE model with the currently available LTNE measures. Standard criteria such as the temperature difference between fluid and solid phases (Abdedou & Bouhadef, 2015; Al-Sumaily et al., 2013; Khashan & Al-Nimr, 2005; Khashan et al., 2006) or the difference between the local fluid temperatures of both models (Hamidi et al., 2019) have a technical meaning, and the transition to a natural environment is difficult. The implications for the heat transport modeling in the field are mostly unknown.

In this study we examine the conditions of forced convective heat transport in natural porous aquifers under which the assumption of LTE applies and determine when it is expected to fail. To achieve this, we systematically compare thermal breakthrough curves (BTCs) calculated using LTE and LTNE models for a range of parameter values that are typical of realistic aquifer conditions. We further develop a new Nusselt number (Nu) correlation to determine the heat transfer coefficient representing the conditions expected in porous aquifers using all available data sets. Finally, we present discrete limits for the conditions under which the commonly used LTE model is applicable when heat transport in porous aquifers is quantified.

2. Method

To investigate the occurrence and impact of LTNE effects on heat transport in porous media, a parameter study with one-dimensional (1-D) numerical LTNE and LTE models is conducted. The notations are given in Appendix A. In a first step, a suitable Nu correlation for porous aquifers to determine the heat transfer coefficient between fluid and solid is derived based on appropriate literature data. Then a numerical model with a step input is used to create thermal BTCs using the LTE and LTNE models. In the last step, the resulting thermal BTCs are evaluated with different methods to quantify LTNE effects. The dominant LTNE parameters are identified through a global sensitivity analysis. More than 50,000 modeling runs are conducted to cover the whole range of possible parameter combinations representative of natural porous aquifers. To evaluate a criterion which allows to easily assess whether the occurrence of LTNE effects is likely, a regression analysis with the sensitive parameters as explanatory variables is conducted.

2.1. Heat Transfer Coefficient

The heat transfer coefficient

$$h_{sf} = \frac{Nu\ \lambda_f}{d_p} \tag{1}$$

is a vital parameter for LTNE models, as it describes the heat transfer rate between the fluid and solid phases. As seen above, h_{sf} depends on Nu, the particle size d_p, and the thermal conductivity of the fluid λ_f

(Wakao et al., 1979). While λ_f and d_p are usually known in ideal packed beds, *Nu* must be estimated using an appropriate correlation which commonly depends on the particle Reynolds number, *Re*, and the Prandtl number, *Pr* (see supporting information Table S1 for examples). Generally, such a correlation is empirically derived from laboratory experiments (Achenbach, 1995; Collier et al., 2004; Naghash et al., 2016; Nie et al., 2011; Shent et al., 1981; Wakao & Kaguei, 1982; Zanoni et al., 2017) or, more recently, by particle resolved direct numerical modeling (Chen & Müller, 2019; Singhal et al., 2017b; Sun et al., 2015; Tavassoli et al., 2015; Zhu et al., 2019). As natural porous aquifers are typified by $Re < 50$ and a porosity (fluid volume fraction) $n < 0.5$, the correlations established by previous studies are covering much broader ranges. Table S1 shows an overview of these correlations and demonstrates that no single model appropriately describes the conditions expected in a porous aquifer. Therefore, a new regression using only the experimental data representative for conditions in porous aquifers ($Re < 50$ and $n < 0.5$) is carried out. We found only one study (Kunii & Smith, 1961) inspecting *Nu* values for very low *Re* ($Re < 0.1$), and their study was disregarded because the mathematical model was criticized by several authors (Gunn & De Souza, 1974; Littman et al., 1968; Wakao et al., 1979). Because the raw data of all of the published experiments were determined with a *Pr* of 0.7–1 (gas), we corrected the *Nu* values based on the correlations of Wakao et al. (1979) and Zhu et al. (2019) (Table S1) using the *Pr* value of 9 (water, 10°C) for each *Nu* of the respective *Re* value *z*:

$$Nu_{cor,\ Re=z} = \left(Nu_{\mathrm{Pr}=9,\ Re=z} - Nu_{\mathrm{Pr}=0.7,\ Re=z}\right) + Nu_{orig,\ Re=z}. \tag{2}$$

$Nu_{orig,\ Re=z}$ gives the originally measured *Nu* value at a *Re* of *z*. To correct for the higher *Pr* of water, the amount of increase of the *Nu* due to the higher *Pr* is added. This amount ($Nu_{\mathrm{Pr}=9,\ Re=z} - Nu_{\mathrm{Pr}=0.7,\ Re=z}$) is calculated with the *Nu* correlation of Wakao et al. (1979) and Zhu et al. (2019) (section S1.1 and Table S1).

Theoretical considerations for heat transfer between a sphere and a fluid flowing around it show that *Nu* must have a minimum value of 2 (Ranz & Marshall, 1952; Shent et al., 1981). As argued, for example, by Nelson and Galloway (1975), lower *Nu* numbers may occur in a packed bed of spheres. In our work, due to the low range of *Pr* expected in groundwater conditions ($Pr^{1/3} \sim 2.08$ at 10°C and $Pr^{1/3} \sim 1.94$ at 20°C), the common dependency of *Nu* on $Pr^{1/3}$ is not resolved. Therefore, following the common dependency of *Nu* on *Re* with a lower limit (see, e.g., Table S1), a correlation of

$$Nu = 1 + aRe^b \tag{3}$$

is fitted to all available data using a and b as free parameters.

In addition to the parameter study of the new correlation, a parameter study is conducted for five (Achenbach, 1995; Singhal et al., 2017b; Wakao et al., 1979; Zanoni et al., 2017; Zhu et al., 2019) other *Nu* correlations, to evaluate the influence of the *Nu* correlation choice.

2.2. LTE and LTNE Models

The heat transport of the fluid and solid phases can be described as a continuous single average temperature field (Equation 4) (Nield & Bejan, 2017) assuming that the temperature difference between the fluid and solid phases within the representative elementary volume is negligible (LTE assumption). The equations are as follows:

$$\frac{\partial T}{\partial t} = D_{l,\ eff}\frac{\partial^2 T}{\partial x^2} - v_{t,\ LTE}\frac{\partial T}{\partial x}, \tag{4}$$

$$D_{l,\ eff} = n\left(\frac{\lambda_f}{\rho_b c_b} + D_l\right) + \frac{(1-n)\lambda_s}{\rho_b c_b}, \tag{5}$$

$$D_l = \beta\left(\frac{\rho_f c_f}{\rho_b c_b} q\right)^2, \tag{6}$$

$$v_{t,\ LTE} = \frac{v_a}{R_{app}} = \frac{n\rho_f c_f}{\rho_b c_b}\frac{q}{n} = \frac{q\rho_f c_f}{\rho_b c_b}. \tag{7}$$

Table 1
Range of Modeling Parameter Values as Used in the Parameter Study Representing Typical Porous Aquifer Ranges (Banks, 2012)

Parameter	Range
Thermal conductivity solid (λ_s)	1.5–8 W m^{-1} K^{-1}
Fluid temperature (T_f)	2–40°C
Seepage velocity (v_a)	1–30 m day^{-1}
Porosity (n)	0.1–0.45
Particle size (d_p)	1 mm to 15 cm
Thermal dispersivity (β)	0.1–10 s^{-1}
Vol. heat capacity solid ($\rho_s c_s$)	$1.5 * 10^6$–$3.5 * 10^6$ J m^{-3} K^{-1}

Note. The thermal dispersivity is based on the power law relationship with the Darcy flux (Rau et al., 2012a).

The first part on the right side of Equation 4 is the effective thermal dispersion coefficient $D_{l,eff}$ (Equation 5) consisting of the thermal diffusivity and thermal mechanical dispersion coefficient D_l (Equation 6) (Rau et al., 2012a). The second part describes the advective heat transport (Equation 7).

When the LTE assumption does not fit, then heat transport can be described with a dispersion particle-based two equation model (LTNE assumption; Equations 8 and 9) (Amiri & Vafai, 1994). The two temperatures are interlinked by a coupling term (Wakao et al., 1979) based on the heat transfer coefficient (Equation 1) and the specific surface area, here assumed for a bed of spherical particles $a_{sf} = (6(1 - n))/d_p$ (Dullien, 1979). The equations are as follows:

$$\frac{\partial T_f}{\partial t} = \left(\frac{\lambda_f}{\rho_f c_f} + D_l\right)\frac{\partial^2 T_f}{\partial x^2} - v_a\frac{\partial T_f}{\partial x} + \frac{h_{sf} a_{sf}}{n\rho_f c_f}\left(T_s - T_f\right), \tag{8}$$

$$\text{zq}\frac{\partial T_s}{\partial t} = \left(\frac{\lambda_s}{\rho_s c_s}\right)\frac{\partial^2 T_s}{\partial x^2} - \frac{h_{sf} a_{sf}}{(1-n)\rho_s c_s}\left(T_s - T_f\right). \tag{9}$$

In the simulations conducted as part of our work, the LTE (Equation 4) and LTNE (Equations 8 and 9) models with the following initial (Equation 10a) and boundary conditions (Equation 10b) were used:

$$T_{f(x,0)} = 0;\ T_{s(x,0)} = 0 \text{ at t} = 0, \tag{10a}$$

$$T_{f(0,t)} = 1;\ \ \frac{\partial T_s}{\partial x} = 0 \text{ at t} > 0,\ \text{x} = 0. \tag{10b}$$

2.3. Numerical Solution and Parameter Study

The LTE and LTNE models explained above were solved using the MATLAB function "pdepe" which utilizes a finite-element, piecewise nonlinear Galerkin/Petrov-Galerkin method with second-order accuracy in space (Skeel & Berzins, 1990). To avoid boundary effects, the model domain was setup with 15 m length. The spatial discretization was 0.0025 m for distances less than 4.5 m (1.5 · maximum distance of interest = 3 m) and increased along the remaining distance. The fine numerical discretization and the chosen input parameter range lead to simulations in which the nodal distance was smaller than the used grain size. While the representative elementary volume is usually larger than the mean grain size in the volume averaging approach (Rau et al., 2014), we do not consider this problematic, as we consider homogenous parameter conditions within the whole model domain. This computationally demanding configuration was chosen as conservative setup to assure mesh independency, but a sensitivity analysis revealed that the results are still acceptable at spatial discretization up to 0.01 m and when reducing the model domain length to 5 m. The time discretization is automatically adapted. A Linux Cluster (at the Leibniz Supercomputing Centre of the Bavarian Academy of Science and Humanities) was utilized to run the simulations in parallel. The numerical solution was validated with analytical solutions (van Genuchten & Alves, 1982; Wakao & Kaguei, 1982) and illustrates good agreement for the LTE and LTNE models (see section S2 for further information).

Table 1 shows the range of values used in our investigation. The parameters are independent of each other, for example, the porosity does not constrain the seepage velocity and so forth. Dependent fluid properties, such as the thermal conductivity λ_f, the density ρ_f, and the specific heat capacity c_f, were calculated from the fluid temperature T_f (Furbo, 2015). *Nu* was computed through the new correlation given by Equation 3 (Figure 2b). The resulting *Re* ranges between 0.015 and 70 with 95% of the simulations within the range of 1 to 50.

To investigate the entire parameter space, first, a uniformly distributed random sample for each independent parameter (Table 1) was created. To decrease the computational cost of the sensitivity analysis, the random parameter sets were extended using Saltelli's (2002) scheme. Then, the dependent fluid parameters were calculated. The number of parameter sets was varied from 48 to 32,000 resulting in 50,608 different parameter

sets for each *Nu* correlation. Each parameter set was used in a model run where a unit step boundary condition was applied to create thermal BTCs for the LTE and LTNE models. The thermal BTCs were analyzed for the distances of 0.5, 1, 2, and 3 m.

2.4. Quantification of LTNE

Three methods were used to quantify the magnitude of the effect of LTNE. Method 1 was newly developed in this study and compared to two existing methods (Methods 2 and 3):

Method 1: Comparison of the difference of effective thermal dispersion and advective thermal velocity between the LTE and LTNE models via the following approach:

1. Simulation of fluid temperature BTC with the LTNE model;
2. Estimation of the effective thermal dispersion coefficient $D_{l,\,eff,\,fit}$ and the advective thermal velocity $v_{t,\,fit}$ from the LTNE calculation (previous step) by fitting the analytical LTE model (van Genuchten & Alves, 1982) (Equation S1) using a standard nonlinear least square fitting procedure;
3. Comparison of the estimated $D_{l,\,eff,\,fit}$ and $v_{t,\,fit}$ from the LTE model with the used $D_{l,\,eff}$ (Equation 5) and $v_{t,\,LTE}$ (Equation 7) in Step 1.

$$LTNE_{method1,\,D_l} = \frac{D_{l,\,eff,\,fit}}{D_{l,\,eff}}, \tag{11}$$

$$LTNE_{method1,\,v} = \frac{v_{t,\,fit}}{v_{t,\,LTE}}. \tag{12}$$

Method 2: Maximum and average temperature difference between the normalized temperature obtained using the LTE model and the fluid temperature obtained using the LTNE model (Hamidi et al., 2019) for each evaluated distance x (N = number of timesteps).

$$LTNE_{method2,\,max,\,x} = max_N\left|T_{LTE,\,x} - T_{LTNE,\,f,\,x}\right|, \tag{13}$$

and

$$LTNE_{method2,\,mean,\,x} = \frac{\sum_1^N\left|T_{LTE,\,x} - T_{LTNE,\,f,\,x}\right|}{N}. \tag{14}$$

Method 3: Maximum and average normalized temperature difference between fluid and solid (Abdedou & Bouhadef, 2015; Al-Sumaily et al., 2013; Khashan et al., 2006; Khashan & Al-Nimr, 2005) obtained using the LTNE model for each distance x:

$$LTNE_{method3,\,max,\,x} = max_N\left|T_{LTNE,\,f,\,x} - T_{LTNE,\,s,\,x}\right|, \tag{15}$$

and

$$LTNE_{method3,\,mean,\,x} = \frac{\sum_1^N\left|T_{LTNE,\,f,\,x} - T_{LTNE,\,\mathrm{s},\,\mathrm{x}}\right|}{N}. \tag{16}$$

2.5. Global Parameter Sensitivity Analysis

To identify the dominant LTNE parameters a global parameter sensitivity was calculated using the function "sobolSalt" as part of the R package "sensitivity" (Iooss et al., 2019). This implements the Monte Carlo estimation of the variance-based sensitivity indices (Sobol indices) of the first and total order for each independent parameter.

3. Results and Discussion

3.1. New Nusselt Correlation

The available *Nu* values found in literature with conditions expected in natural porous aquifers ($Re < 50$, $n < 0.5$) are shown in Figure 1. The original *Nu* values determined with gas as fluid ($Pr = 0.7$) were adapted for water as fluid ($Pr = 9$) using the *Nu* correlations and Equation 2 (see section S1 for further information).

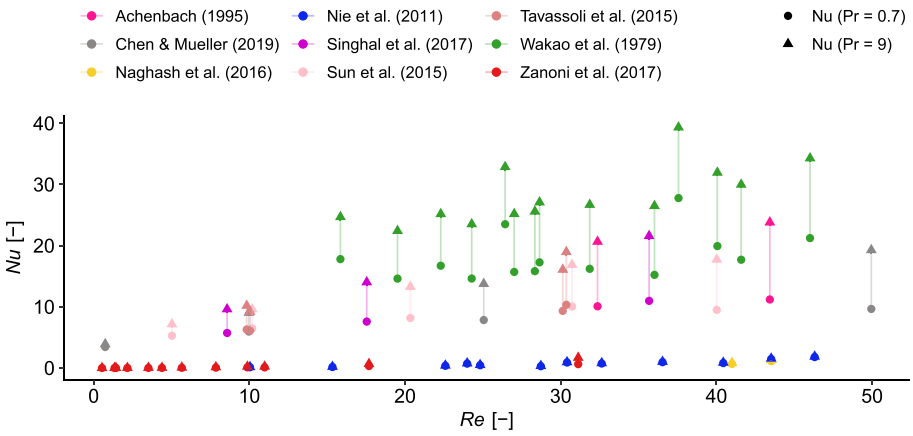

Figure 1. Summary of literature-based Nusselt values for the Reynolds ($Re < 50$) and porosity ($n < 0.5$) range expected in natural porous aquifers. As most studies were conducted with gas as a fluid, the Nusselt numbers were corrected for the Prandtl number of water using Equation 2.

Some correlations and data (Naghash et al., 2016; Nie et al., 2011; Zanoni et al., 2017) result in very low *Nu* numbers for the investigated *Re* range (Figure 2a). A reason for the discrepancy in *Nu* values between some publications (Naghash et al., 2016; Nelson & Galloway, 1975; Nie et al., 2011; Zanoni et al., 2017) (first group) and other studies (Achenbach, 1995; Singhal et al., 2017b; Sun et al., 2015; Wakao et al., 1979; Zhu et al., 2019) (second group) is not obvious, and therefore, the unrealistic data for porous aquifers from the first group were not included in our regression. The new regression based on the available data and Equation 3 is shown in Figure 2. This correlation with best fit values $a = 3.1$ and $b = 0.57$ is used in all of the presented analysis.

3.2. Comparison of Thermal BTCs Obtained From the LTE and LTNE Models

Significant differences between the modeled thermal BTCs calculated using the LTE and LTNE models can be found within the assumed parameter ranges representative of the conditions in porous aquifers. As an example, Figure 3 highlights the thermal BTCs obtained from the LTE and LTNE models for particle sizes (<0.5 cm) with slow flow velocities (<2 m day^{-1}) at the lower end of the investigated parameter range (Figures 3a–3c) and for large particles sizes (>7.5 cm) with high flow velocities (>20 m day^{-1}) (Figures 3d–3f). Furthermore, the three different methods used to evaluate the degree of LTNE are

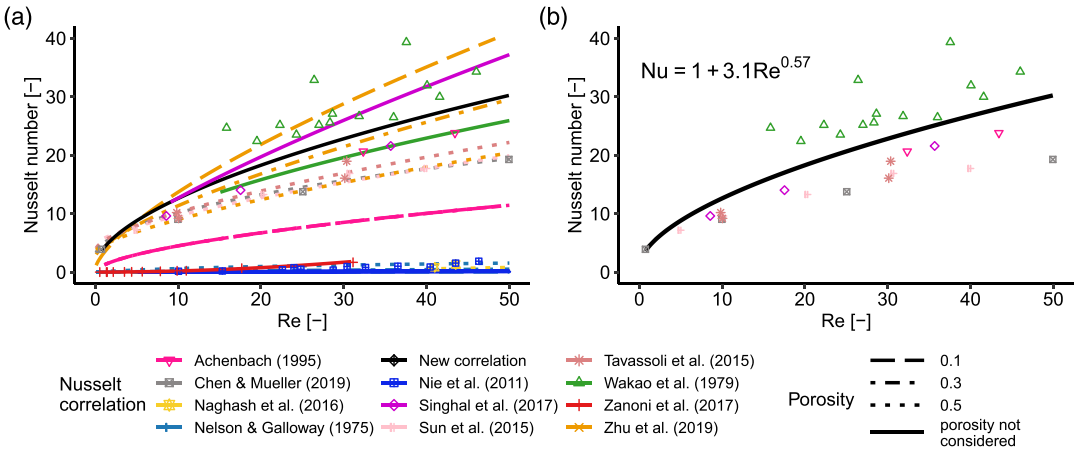

Figure 2. (a) Comparison of different Nusselt correlations with the respective data points. (b) Used data for the new correlation based on the Prandtl corrected Nusselt values of published experimental data.

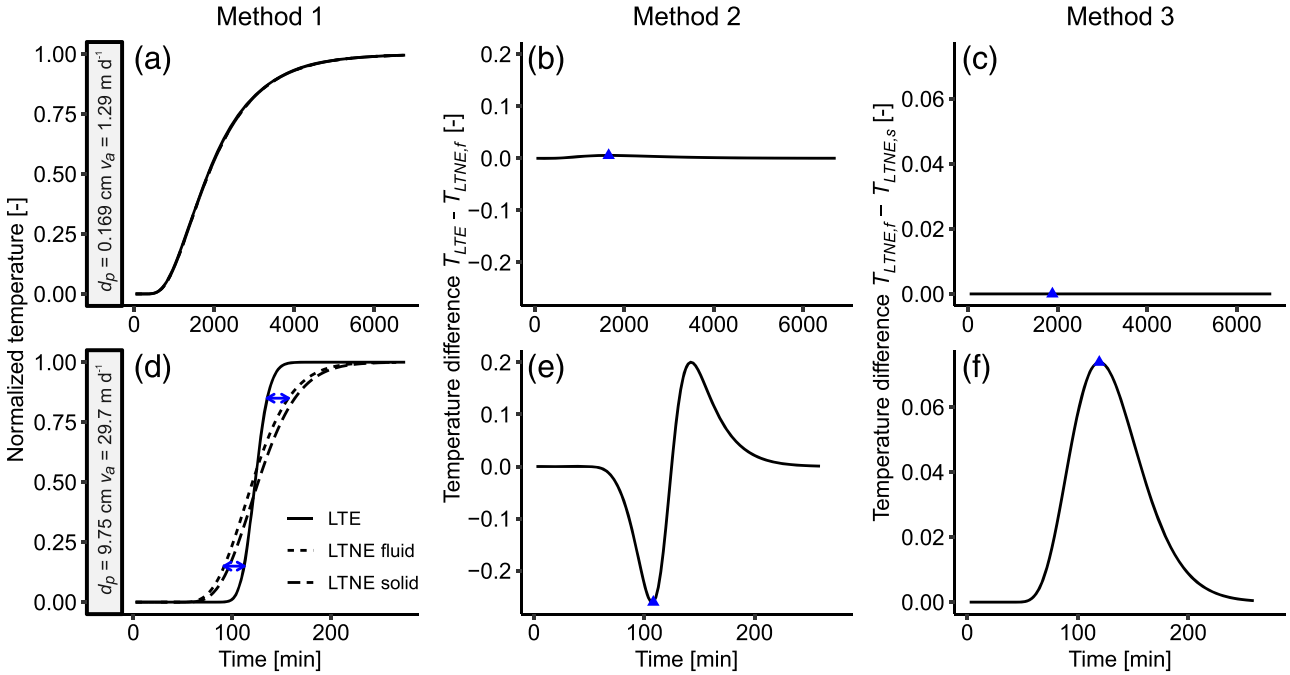

Figure 3. Example of thermal BTCs illustrating the three different methods used to quantify LTNE. (a)–(c) summarize conditions with small particles sizes d_p and low flow velocities v_a. (d)–(f) display large particle sizes and high flow velocity conditions. Method 1 uses a normalized temperature BTC. The degree of LTNE is measured as the difference in thermal dispersion (blue arrows) and advective thermal velocity between the LTNE fluid temperature and the LTE model. Method 2 uses the temperature difference between the normalized LTE temperature and normalized LTNE fluid temperature. Method 3 measures the maximum and average temperature difference between the normalized solid and fluid temperatures. The blue triangles indicate the position of the maximum absolute values.

illustrated. For low flow velocities and small particle sizes, the LTE and LTNE models result in similar (visually the same) thermal BTCs regarding effective dispersion and advective thermal velocity (Method 1). The computed normalized temperature differences between the LTE and LTNE fluid temperature (Method 2) and LTNE fluid and solid temperature (Method 3) are very low (<0.005). In contrast, in the simulations for large particle sizes and high flow velocities, the thermal BTCs from the two models differ significantly. The solid and fluid temperature of the LTNE model is noticeably more dispersed (Method 1), and significant temperature differences between the LTE temperature and LTNE fluid temperature (Method 2) as well as solid and fluid temperature (Method 3) can be observed.

3.3. Influence of the Nusselt Correlation

To investigate the influence of the *Nu* correlation choice, the parameter study was extended to the *Nu* correlations suggested by Zanoni et al. (2017) as well as four others (Achenbach, 1995; Singhal et al., 2017b; Wakao et al., 1979; Zhu et al., 2019). For the *Nu* correlation by Zanoni et al. (2017) (very low *Nu* values), nearly all tested conditions lead to strong LTNE effects (see Figures S4 and S5). As an example, Figures 4a and 4b show the thermal BTCs using different *Nu* correlations for the identical conditions as in Figures 3a–3c. It is clear that the fluid temperature front calculated using the LTNE model with the *Nu* correlation of Zanoni et al. (2017) shows no significant retardation compared to the fluid front. By contrast, the solid phase temperature increases much slower due to the very low heat exchange between the fluid and solid phases as caused by the low *Nu* values from this correlation (see Table S2 for values of *Nu*). Both fluid and solid BTCs obtained from the LTNE model for the *Nu* correlation of Zanoni et al. (2017) differ significantly from the temperature calculated using the LTE model. In fact, fitting the analytical LTE model to the fluid temperature BTC obtained from the LTNE model fails to achieve a satisfactory result (see Figure S6). All other *Nu* correlations lead to similar BTCs. This shows that *Nu* correlations leading to very low *Nu* numbers are not suitable for natural conditions when simply adjusting the *Pr* to a value appropriate for water.

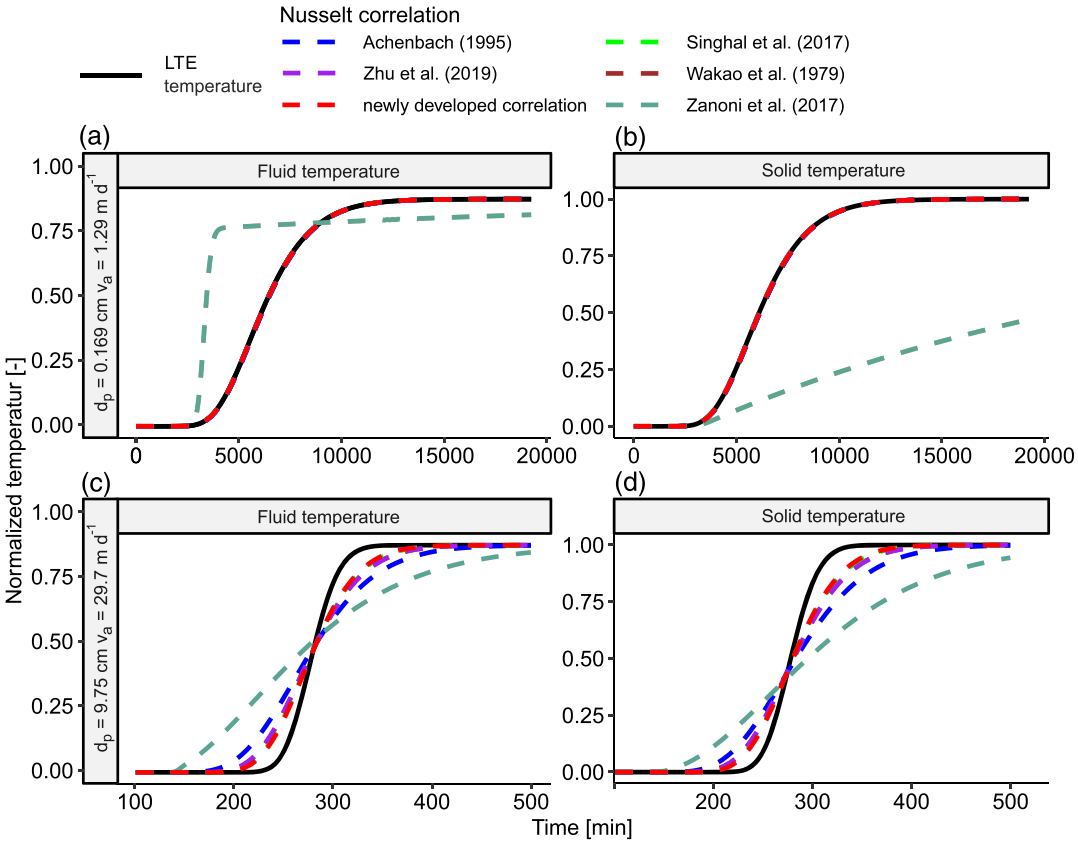

Figure 4. Comparison of the thermal breakthrough curves for different *Nu* correlations for identical parameter sets as in Figure 3. In conditions with small particles sizes d_p and low flow velocities v_a (a and b), the breakthrough curves for the second group of *Nu* correlations are identical and also match the LTE temperature. For conditions with large particle sizes and high flow velocity conditions (c and d), the breakthrough curves for all *Nu* correlations differ significantly from the LTE model.

In conditions with large particle sizes and high seepage velocities (Figures 4c and 4d), all BTCs of the different *Nu* correlations differ from the LTE model showing higher dispersion while slightly differing from each other. Therefore, the general outcome that LTNE conditions lead to higher thermal dispersion is nearly independent of the choice of the *Nu* correlation (see also Figure S7).

3.4. Analysis of the Parameter Sensitivity

The parameter sensitivity analysis reveals that when evaluating all three methods, the most sensitive parameters are the seepage velocity, the particle size, and the porosity. The least sensitive parameters are found to be the fluid temperature, the volumetric heat capacity of the solid, and the thermal dispersivity. The full details of the sensitivity analysis are given in section S4. In many engineering applications, the ratio of fluid to solid phase thermal conductivities is reported as an important LTE criterion (Dehghan et al., 2014; Lee & Vafai, 1998; Minkowycz et al., 1999). The ratio between the thermal conductivity of water (Huber et al., 2012) and common aquifer materials (Côté & Konrad, 2005) is usually in the range ~0.1–0.5. The differences between the thermal conductivities in engineering applications with air as fluid and metals as a solid phase span a much broader range. We believe that our analysis did not find this to cause sensitivity because of the limited range of thermal conductivities expected in aquifer settings, as was the focus in our study.

3.5. The Influence of LTNE Effects on the Advective Thermal Velocity

The modeled against the fitted thermal velocity is shown in Figure 5a, highlighting an excellent fit ($R^2 > 0.99$) with generally very small differences (for 95% of the simulations, the deviation is smaller

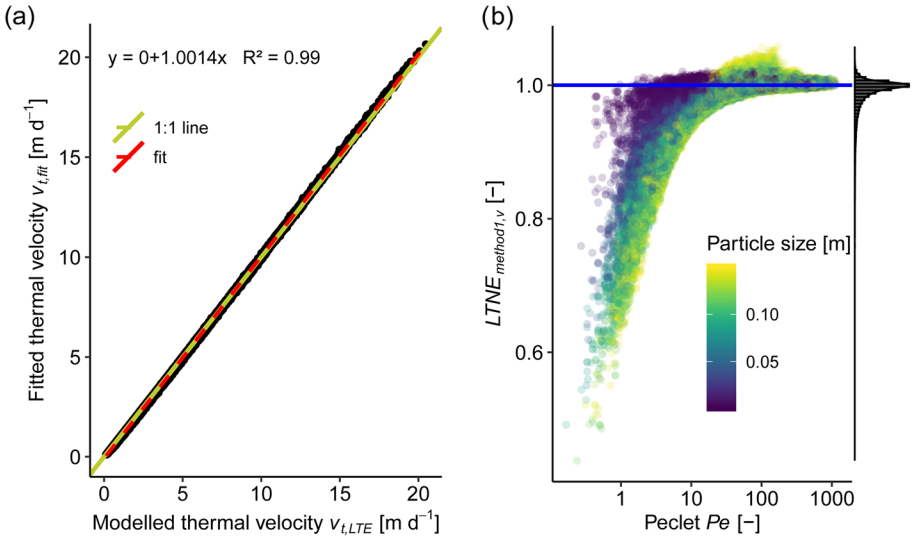

Figure 5. (a) The differences between the fitted advective thermal velocity and the modeled advective thermal velocity are very small for most simulations. For 95% of the simulations, the deviation is smaller than 5%. The fitted velocity deviates at very high velocities by a small amount (<5%) from the modeled advective thermal velocity. This shows that the influence of LTNE effects on the advective thermal velocity is generally very small. (b) For a small part of the simulations at low Peclet numbers in combination with large particle sizes, the fitted velocity is smaller than the modeled thermal velocity. This deviation at low Peclet numbers, representing conduction dominated situations at small flow distances, is contributed to the differences in the boundary conditions immanent in the chosen LTE and LTNE models.

than 5%). A small number of simulations at low Peclet numbers and large particle sizes deviate from the expected thermal advective velocity (Figure 5b). Aside from these conditions, the influence of LTNE effects on the advective velocity is generally very low. The fitted flow velocities exceed the modeled velocities slightly (<5%) at very high velocities. The results also illustrate that this is not flow distance dependent, as the correlations are similar for all investigated distances (Figure S10). These observations are in agreement with a recent study (Gossler et al., 2019) which experimentally investigated possible LTNE effects. No significant influence on the advective thermal velocity could be observed within the analyzed range of seepage velocities expected in gravel aquifers (5–50 m day^{-1}). In a numerical study, Roshan et al. (2014) investigated the influence of LTNE effects on velocity estimates from the damping and phase shifting of the diel temperature signal with depth in a streambed for flux conditions leading to $0.001 < Re < 0.01$. They come to an opposite conclusion, stating that LTNE effects are limited to very slow flow velocities but can lead to velocity deviations up to a factor of 150. A possible explanation of these findings is their choice of the *Nu* correlation which leads to very low *Nu* numbers at low flow velocities but increases significantly at higher velocities. Furthermore, the mathematical model used to derive the *Nu* values (Kunii & Smith, 1961) on which the correlation of Roshan et al. (2014) is based was criticized by several authors (Gunn & De Souza, 1974; Littman et al., 1968; Wakao et al., 1979).

3.6. The Influence of LTNE Effects on Thermal Dispersion

In contrast to the advective thermal velocity, the effective thermal dispersion can be significantly influenced by LTNE effects. We evaluate that an increase by a factor of over 30 ($LTNE_{method1,\,D_l}$) is possible within the range of parameters investigated in this study (Figure 6). Increasing flow velocities and particle sizes also lead to increasing LTNE effects and, consequently, to a higher effective thermal dispersion. Similar results are obtained for all investigated distances (Figure S11). To elucidate the conditions under which this increase in thermal dispersion can be expected, the LTNE effects on thermal dispersion have been categorized in Table 2. As the thermal dispersion is generally an uncertain parameter in modeling, we considered an increase up to 50% as within the usual uncertainty range. An increase above a factor of 10 is considered as highly influenced by LTNE effects. Following this categorization and the grain

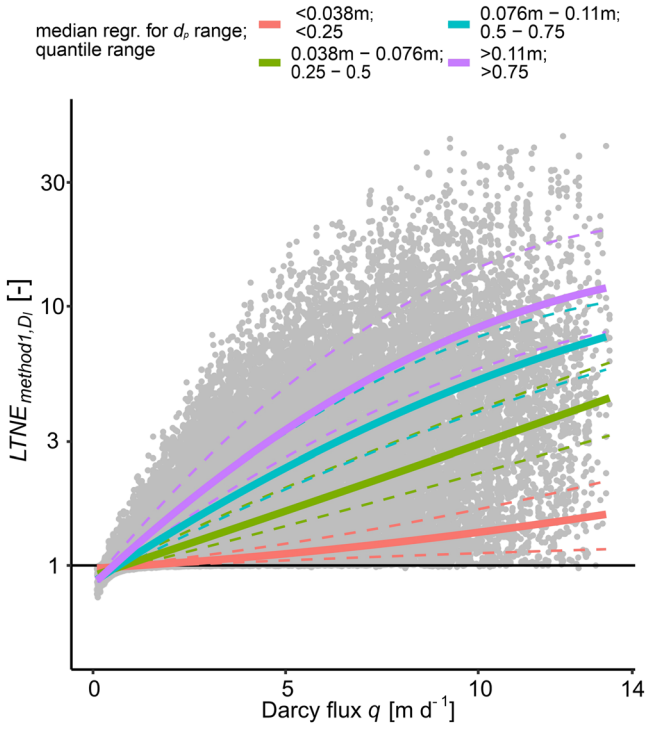

Figure 6. The influence of Darcy flux on the normalized deviation of the thermal dispersion difference $(LTNE_{method1,\,D_l})$ caused by LTNE effects. Each gray dot is the result of one simulation. The solid colored lines show the smoothed median values (dashed lines 0.25/0.75 quartile) of the normalized dispersion deviations for groups of simulations with different particle size ranges. Larger particle sizes and higher Darcy fluxes lead to higher LTNE effects resulting in a significant increase in the thermal dispersion.

size-based aquifer types according to Table 2, we reveal that LTNE effects can be expected in gravel aquifers with high Darcy fluxes (Figure 7). Furthermore, we identify the following threshold values considering all combinations of parameters for which no significant LTNE effects ($LTNE_{method1,\,D_l} < 1.5$) could be observed: If either the particle size is <7 mm or the seepage velocity is <1.6 m day^{-1}, no significant LTNE effects ($LTNE_{method1,\,D_l} < 1.5$) should be expected. Two previous laboratory studies (Bandai et al., 2017; Gossler et al., 2019) observed increasing thermal dispersion values with increasing particle sizes and suspected LTNE effects as the cause for this. Our results confirm the assumption that LTNE effects can significantly enhance the effective thermal dispersion coefficient.

3.7. Comparison of the Methods to Quantify LTNE Effects

The comparison of the results of the three methods for all simulations shows a significant relationship between them (Figure 8). Yet, for some parameter settings (low *Pe* and large d_p), the differences between the LTE and fluid LTNE temperatures ($LTNE_{method2}$) are large, while the differences between solid and fluid temperature ($LTNE_{method3}$) are close to zero. These findings are in accordance with the results of some other studies (Hamidi et al., 2019; Rees et al., 2008) which showed that LTE and LTNE models can differ even if the temperature differences between the fluid and solid phase are nearly equal. Interestingly, while $LTNE_{method1,Dl}$ does not capture these LTNE effects, $LTNE_{method1,v}$ shows a strong correlation with $LTNE_{method2,\,max}$ (Figure 8b). These deviations are limited to conditions of low *Pe* numbers (Figures 5b and 8b).

A possible explanation for these discrepancies at low *Pe* is the differences in the boundary conditions between the LTE and LTNE models. When trying to model a scenario in which a hot or cold fluid is injected into a porous medium, the boundary condition necessary for the LTE model and the assumption inherent to the LTE model induce that under conduction-dominated conditions (low *Pe*), the thermal conductivity of the solid phase also contributes significantly to heat transport at the boundary (see Equations 4 and 5). The LTNE model allows to set more appropriate boundary conditions, allowing to only affect the fluid phase at the boundary.

3.8. Criterion to Estimate LTNE Conditions

To estimate if LTNE effects are likely to occur in porous aquifers, we use the four most sensitive parameters, particle size d_p, porosity n, seepage velocity v_a, and thermal conductivity of the solid phase λ_s, as explanatory variables to derive a new equation in a two-step regression procedure. First, to find the best model formula, an exhaustive screening approach with the R package "glmulti" (Calcagno & de Mazancourt, 2010) was applied on the normalized (ordered quantile normalization; Peterson & Cavanaugh, 2019) $LTNE_{method1,\,D_l}$ value and the scaled explanatory variables (min-max normalization) (for further details, refer to

Table 2
Categorization of the LTNE Effects and Typical Aquifer Types

Aquifer type	Seepage velocity (m day^{-1})	Particle size (mm)	Porosity (–)	LTNE categorization	Quasi-LTE	Low LTNE	Medium LTNE	High LTNE
Sand	1–3	1–2	0.1–0.2	$LTNE_{method1,\,Dl} = \frac{D_{l,\,eff,\,fit}}{D_{l,\,eff}}$	<1.5	1.5–3	3–10	>10
Sand- gravel	2–10	1.5–30	0.15–0.3					
Gravel	5–30	20–150	0.25–0.45					

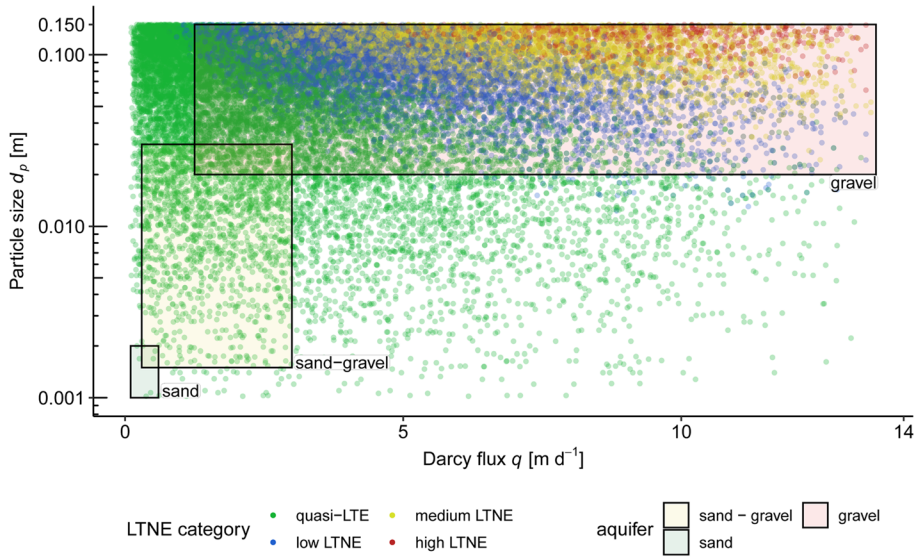

Figure 7. Categorized LTNE effects based on Darcy flux and particle size. Increased thermal dispersion due to LTNE effects is mainly expected for conditions with high flow velocities and large grain sizes like gravel aquifers.

section S6). In other words, the abovementioned explanatory variables are used to predict the value of $LTNE_{method1,\,D_l}$. The value of $LTNE_{method1,\,D_l}$, predicted by the regression, is called $LTNE_{cat}$. All possible models including pairwise interactions were considered up to a maximum number of seven terms. The selection was based on Bayesian information criterion which penalizes models with higher number of parameters to prevent overfitting (Schwarz, 1978). The model formula in Equation 17 with six terms shows the best results concerning limited complexity and adequate accuracy (adjusted $R^2 = 0.89$). In order to enable a practical application, the regression coefficients were determined by applying this model to the original data (not normalized and scaled) (adjusted $R^2 = 0.64$) resulting in

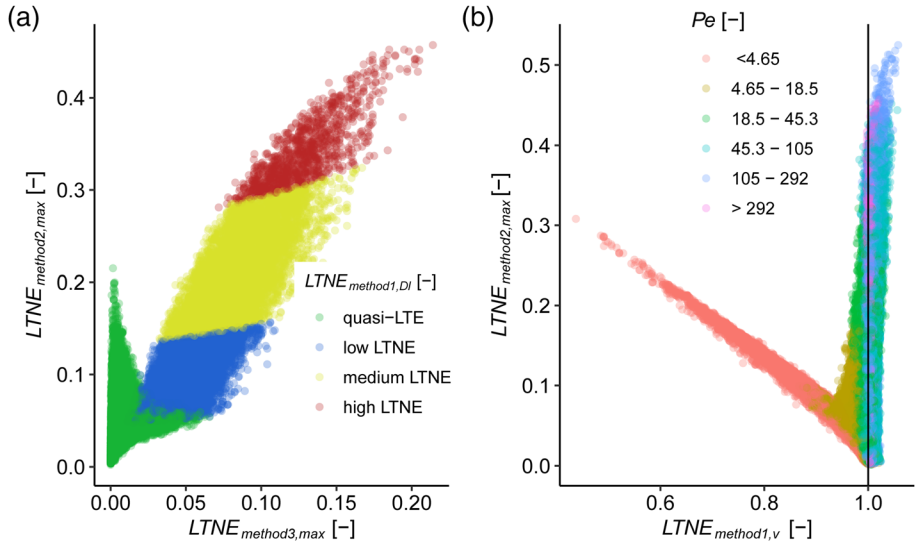

Figure 8. Relationship between the different LTNE quantification methods. (a) While the methods show a significant correlation between them, $LTNE_{method2,\,max}$ detects increased differences between the LTE and LTNE fluid temperature for low Péclet conditions in which the difference between fluid and solid temperature ($LTNE_{method3,\,max}$) is negligible and the dispersion is not significantly increased ($LTNE_{method1,\,Dl}$). b) $LTNE_{method1,v}$ shows an overestimation of the advective velocity of the LTE model for these low Péclet conditions and a correlation with $LTNE_{method2,\,max}$.

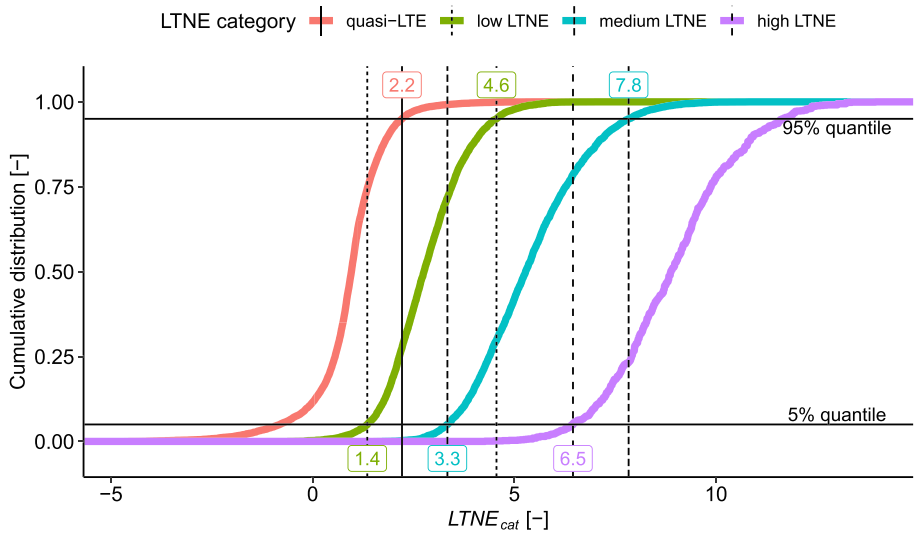

Figure 9. Cumulative distribution of the LTNE categories based on Table 2 and the predicted values by Equation 17. The 5% and 95% quantile values of $LTNE_{cat}$ of the different LTNE categories are used to determine the boundary values of the LTNE categories (Table 3).

$$LTNE_{cat} = 0.42 - 0.04v_a - 1.45n + 0.21\lambda_s + 2.15d_p v_a + 118.11d_p n - 8.38\lambda_s d_p. \quad (17)$$

The predicted value $LTNE_{cat}$ (Equation 17) was compared with the associated LTNE category (Table 2) for each simulation in a cumulative distribution plot (Figure 9). The boundaries of the categories (Table 3 and Figure 9) are based on the 5% and 95% quantiles of this cumulative distribution. This can be viewed as a probability measure, for example, if $LTNE_{cat}$ is <1.4, it is likely that no LTNE effects occur. Ninety-five percent of the simulations which show low LTNE effects are above this value. No simulation with medium or high LTNE effects results in an $LTNE_{cat} < 1.4$. If $LTNE_{cat}$ is in the low LTNE-medium LTNE range (3.3–4.6), both categories are equally possible, as simulation with parameter sets resulting in this range can be within both categories (Figure 9). The accuracy of this approach is reasonable, as $LTNE_{cat}$ gives only a qualitative assessment of the LTNE conditions.

3.9. Limitations of the Used Approach

Our study focuses on a 1-D setup with homogenous parameter settings in each simulation to investigate LTNE effects. Even though most of the parameter settings expected in porous aquifers are covered, the influence of macroscopic heterogeneity on LTNE effects remains unclear. A recent publication investigated LTE and LTNE approaches for fractured porous media (Hamidi et al., 2019). They showed that high permeability and porosity contrasts can lead to significant LTNE effects resulting in a difference of up to 7% in local fluid temperatures. This indicates that macroscopic heterogeneity could additionally increase LTNE effects.

Furthermore, we used the arithmetic mean particle size as a referential particle size in our simulations. The sensitivity analysis showed that the particle size is a highly influential parameter for LTNE effects. Similarly, Heinze and Blöcher (2019) revealed that the particle size is a crucial parameter for LTNE effects during infiltration processes. For transferring the results to aquifers with unsorted grain size distributions, further research is necessary to reveal if, for instance, a representative grain size would be suitable. Candidates are statistical grain size values such as the geometric or harmonic means as common for calculation of thermal or hydraulic conductivity.

Table 3
Categories of the LTNE Effects and the Corresponding Values of $LTNE_{cat}$

LTNE category	$LTNE_{cat}$	Boundaries based on quantiles
Quasi-LTE	<1.4	<5% quantile low LTNE
Quasi-LTE-low LTNE	1.4–2.2	5% quantile low LTNE-95% quantile quasi LTE
Low LTNE	2.2–3.3	95% quantile quasi LTE-5% quantile medium LTNE
Low LTNE-medium LTNE	3.3–4.6	5% quantile medium LTNE-95% quantile low LTNE
Medium LTNE	4.6–6.5	95% quantile low LTNE-5% quantile high LTNE
Medium LTNE-high LTNE	6.5–7.8	5% quantile high LTNE-95% quantile medium LTNE
High LTNE	>7.8	>95% quantile medium LTNE

Another assumption of our study is that we consider most parameters independent of each other (see section 2.3). Certainly, some parameters like particle size and porosity can be correlated (e.g., Urumović & Urumović, 2014), but these correlations depend on many influences like grain size distribution, shape of the grains, and compaction. Therefore, we have not elaborated further on which conditions are more or less frequent in natural aquifers and rather provide the full range of parameter combinations.

3.10. Implications for Heat Transport Modeling and Interpretation

The increased thermal dispersion caused by LTNE under certain conditions can have significant consequences for the modeling and management of geothermal groundwater use, such as groundwater-based heat pump systems, which cycle groundwater by operating extraction and injection well doublets. With a steady increase of such systems leading to densely used aquifers (Pophillat et al., 2020), there is a growing need for reliable prediction of the induced thermal plumes (Böttcher et al., 2019; Epting et al., 2017; Ferguson, 2009; Hähnlein et al., 2013; Herbert et al., 2013). To delineate a thermal range or a thermally affected zone in an aquifer, the value for thermal dispersion is of crucial importance (Molina-Giraldo et al., 2011; Park et al., 2015, 2018; Pophillat et al., 2020). Consequently, the processes that determine its magnitude must be well understood. For example, we expect that LTNE effects can occur even in aquifers with low natural seepage water velocities as the flow velocity increases significantly toward injection and extraction wells (Park et al., 2015). Furthermore, the highly transient operation typical for groundwater-based heat pump systems (Muela Maya et al., 2018) can enhance the effects of LTNE (Minkowycz et al., 1999). Therefore, an increase in effective thermal dispersion due to LTNE effects should be carefully considered under the conditions depicted in Figure 7. Thermal nonequilibrium potentially also affects the storage of thermal energy in aquifers composed of large particle sizes. The increased spreading of the thermal front in the fluid phase due to an incomplete storage in the solid phase leads to an initially lower energy density in the area of interest than is expected when a LTE model is used. Finally, when using heat as a tracer, the aim is often to quantify fluxes (Irvine et al., 2015, 2017; Rosenberry et al., 2015) or use the advective part for an inversion of the hydraulic conductivity field (Somogyvári & Bayer, 2017; Somogyvári et al., 2016). In dynamic interfaces with surface-water bodies, such as when aquifers interact with rivers, groundwater can reach velocities up to 10 m day^{-1} and higher (e.g., Angermann et al., 2012; Cremeans et al., 2018; Rau et al., 2014). These systems are possibly influenced by LTNE effects. As the groundwater velocities for interactions with lakes are usually well below 1 m day^{-1} (Rosenberry et al., 2015), the LTE assumption is mostly applicable for these conditions. Only at low *Pe* numbers in combination with large particle sizes an LTE model can overestimate the advective thermal velocity. Even in conditions with strong LTNE effects, for some of these cases, the LTE model is appropriate (Figure 7) because the LTNE effects do not significantly influence the advective thermal velocity at advection-dominated conditions.

4. Conclusion

The limitations of the LTE assumption in heat transport modeling for natural porous aquifers have been investigated by an extensive 1-D parameter study comparing thermal BTCs of LTE and LTNE models. A new correlation to determine the Nusselt number based on available literature data tailored to porous aquifers was derived. As all available data on *Nu* are determined with air as fluid, more laboratory studies measuring the heat transfer with water as a fluid are required.

While LTNE effects do not occur for grain sizes smaller than 7 mm or for flow velocities that are slower than 1.6 m day^{-1}, LTNE effects can occur within the conditions expected in porous aquifers like gravel aquifers with high flow velocities and large grain sizes. The effective thermal dispersion can be increased by a factor of over 30 caused by LTNE effects. The advective thermal velocity is not significantly influenced even in conditions with strong LTNE effects. Only at low *Pe* conditions in combination with large particle sizes, the LTE model can lead to an overestimation of the advective thermal velocity. A criterion to predict if LTNE conditions will occur is developed based on the most influential properties, the porous media particle size, seepage velocity, porosity, and thermal conductivity of the solid phase. Our results can be used as a guide toward more accurate modeling of heat transport in natural porous media.

Appendix A: Nomenclature

Nomenclature of the used notations in the article and the supporting information.

Table A1
Nomenclature

Parameter	Units	Description	Parameter	Units	Description
a_{sf}	(m^{-1})	specific surface area solidfluid per unit volume	T_{inj}	(K)	injection temperature
c	(J kg^{-1} K^{-1})	Specific heat capacity	T	(−)	Normalized temperature (see Equation S1)
$D_{l,eff}$	(m^2 s^{-1})	Effective longitudinal thermal dispersion (Equation 5)	v_a	(m s^{-1})	Seepage velocity
$D_{l,eff,fit}$	(m^2 s^{-1})	Effective thermal dispersion fitted with analytical LTE model (Equation S1)	v_i		see Equation S7
$D_l = \beta \left(\frac{\rho_f c_f}{\rho_b c_b} q\right)^2$	(m^2 s^{-1})	Longitudinal thermal mechanical dispersion model	v_t	(m s^{-1})	Advective thermal velocity
d_p	(m)	Particle diameter	$v_{t,fit}$	(m s^{-1})	Advective thermal velocity fitted with analytical LTE model (Equation S1)
h_{sf}	(W m^{-2} K^{-1})	Heat transfer coefficient	x	(m)	Distance
$LTNE$	(−)	Measure to quantify degree of local-thermal nonequilibrium	β	(s^{-1})	Thermal dispersivity
$LTNE_{cat}$	(−)	Criterion to estimate degree of LTNE (see Equation 17)	λ	(W m^{-1} K^{-1})	Thermal conductivity
m_i		ith root of Equation S5	η	(kg m^{-1} s^{-1})	Dynamic viscosity
n	(−)	Porosity, fluid volume fraction	ρ	(kg m^{-3})	Specific density
N	(−)	Number of timesteps	τ	(s)	Time period for analytical solution of LTNE model (Equations S2–S8); long enough to reach $T = T_{inj}$
$Nu = \frac{h_{sf} d_p}{\lambda_f}$	(−)	Nusselt number	Subscripts:		
P_i		ith root of Equations S6a–S6d	s		Solid
$Pe = \frac{qL}{D_{l,\,eff}}$	(−)	Thermal Péclet number L as characteristic length (flow distance)	f		Fluid
$Pr = \frac{\eta c_f}{\lambda_f}$	(−)	Prandtl number	b		Bulk saturated porous media
q	(m s^{-1})	Specific discharge	LTE		Local thermal equilibrium model
R_{app}	(−)	Expected thermal retardation (Equation 7)	$LTNE$		Local thermal nonequilibrium model
$Re = \frac{\rho_f v_a d_p}{\eta}$	(−)	Reynolds number	$method$		Method used to quantify LTNE
t	(s)	Time	$analytical$		Modeled with analytical model
T_0	(K)	Initial temperature	$numerical$		Modeled with numerical model
T_{degree}	(K)	Temperature			

Data Availability Statement

The result data set and the R and Matlab scripts used to create the data set of this study are available at the mediaTum data repository (institutional repository of the Technical University of Munich) (https://mediatum.ub.tum.de/1543886; 10.14459/2020md1543886).

Acknowledgments
This research was conducted within the GeoPot-project, which is financed by the Bavarian State Ministry of the Environment and Consumer Protection. We thank the three anonymous reviewers and the associated editor for their detailed assessment and very constructive comments.

References

Abdedou, A., & Bouhadef, K. (2015). Comparison between two local thermal non equilibrium criteria in forced convection through a porous channel. *Journal of Applied Fluid Mechanics*, *8*(3), 491–498. https://doi.org/10.18869/acadpub.jafm.67.222.22233

Achenbach, E. (1995). Heat and flow characteristics of packed beds. *Experimental Thermal and Fluid Science*, *10*(1), 17–27. https://doi.org/10.1016/0894-1777(94)00077-L

Al-Nimr, M. A., & Abu-Hijleh, B. A. (2002). Validation of thermal equilibrium assumption in transient forced convection flow in porous channel. *Transport in Porous Media*, *49*(2), 127–138. https://doi.org/10.1023/A:1016072713296

Al-Sumaily, G. F., Sheridan, J., & Thompson, M. C. (2013). Validation of thermal equilibrium assumption in forced convection steady and pulsatile flows over a cylinder embedded in a porous channel. *International Communications in Heat and Mass Transfer*, *43*, 30–38. https://doi.org/10.1016/j.icheatmasstransfer.2013.01.009

Amiri, A., & Vafai, K. (1994). Analysis of dispersion effects and non-thermal equilibrium, non-Darcian, variable porosity incompressible flow through porous media. *International Journal of Heat and Mass Transfer*, *37*(6), 939–954. https://doi.org/10.1016/0017-9310(94)90219-4

Amiri, A., & Vafai, K. (1998). Transient analysis of incompressible flow through a packed bed. *International Journal of Heat and Mass Transfer*, *41*(24), 4259–4279. https://doi.org/10.1016/S0017-9310(98)00120-3

Angermann, L., Krause, S., & Lewandowski, J. (2012). Application of heat pulse injections for investigating shallow hyporheic flow in a lowland river. *Water Resources Research*, *48*, W00P02. https://doi.org/10.1029/2012WR012564

Bakker, M., Caljé, R., Schaars, F., Van Der Made, K. J., & De Haas, S. (2015). An active heat tracer experiment to determine groundwater velocities using fiber optic cables installed with direct push equipment. *Water Resources Research*, *51*, 2760–2772. https://doi.org/10.1002/2014WR016632

Bandai, T., Hamamoto, S., Rau, G. C., Komatsu, T., & Nishimura, T. (2017). The effect of particle size on thermal and solute dispersion in saturated porous media. *International Journal of Thermal Sciences*, *122*, 74–84. https://doi.org/10.1016/j.ijthermalsci.2017.08.003

Banks, D. (2012). *An introduction to thermogeology: Ground source heating and cooling* (2nd ed.). Oxford UA: Wiley-Blackwell. https://doi.org/10.1002/9781118447512

Bekele, E., Patterson, B., Toze, S., Furness, A., Higginson, S., & Shackleton, M. (2014). Aquifer residence times for recycled water estimated using chemical tracers and the propagation of temperature signals at a managed aquifer recharge site in Australia. *Hydrogeology Journal*, *22*(6), 1383–1401. https://doi.org/10.1007/s10040-014-1142-0

Böttcher, F., Casasso, A., Götzl, G., & Zosseder, K. (2019). TAP—Thermal aquifer potential: A quantitative method to assess the spatial potential for the thermal use of groundwater. *Renewable Energy*, *142*, 85–95. https://doi.org/10.1016/j.renene.2019.04.086

Calcagno, V., & de Mazancourt, C. (2010). glmulti: An R package for easy automated model selection with (generalized) linear models. *Journal of Statistical Software*, *34*(12), 1–29. https://doi.org/10.18637/jss.v034.i12

Chen, Y., & Müller, C. R. (2019). Lattice Boltzmann simulation of gas-solid heat transfer in random assemblies of spheres: The effect of solids volume fraction on the average Nusselt number for Re ≤ 100. *Chemical Engineering Journal*, *361*, 1392–1399. https://doi.org/10.1016/j.cej.2018.10.182

Collier, A. R., Hayhurst, A. N., Richardson, J. L., & Scott, S. A. (2004). The heat transfer coefficient between a particle and a bed (packed or fluidised) of much larger particles. *Chemical Engineering Science*, *59*(21), 4613–4620. https://doi.org/10.1016/j.ces.2004.07.029

Côté, J., & Konrad, J. M. (2005). A generalized thermal conductivity model for soils and construction materials. *Canadian Geotechnical Journal*, *42*(2), 443–458. https://doi.org/10.1139/t04-106

Cremeans, M. M., Devlin, J. F., McKnight, U. S., & Bjerg, P. L. (2018). Application of new point measurement device to quantify groundwater-surface water interactions. *Journal of Contaminant Hydrology*, *211*, 85–93. https://doi.org/10.1016/j.jconhyd.2018.03.010

Dehghan, M., Valipour, M. S., & Saedodin, S. (2014). Perturbation analysis of the local thermal non-equilibrium condition in a fluid-saturated porous medium bounded by an iso-thermal channel. *Transport in Porous Media*, *102*(2), 139–152. https://doi.org/10.1007/s11242-013-0267-2

Dullien, F. A. L. (1979). *Porous media: Fluid transport and pore structure* (Vol. 21, pp. 177–178). New York, NY: Academic Press. https://doi.org/10.1016/0300-9467(81)80049-4

Epting, J., García-Gil, A., Huggenberger, P., Vázquez-Suñe, E., & Mueller, M. H. (2017). Development of concepts for the management of thermal resources in urban areas—Assessment of transferability from the Basel (Switzerland) and Zaragoza (Spain) case studies. *Journal of Hydrology*, *548*, 697–715. https://doi.org/10.1016/j.jhydrol.2017.03.057

Ferguson, G. (2009). Unfinished business in geothermal energy. *Ground Water*, *47*(2), 167. https://doi.org/10.1111/j.1745-6584.2008.00528.x

Furbo, S. (2015). Using water for heat storage in thermal energy storage (TES) systems. In L. F. Cabeza (Ed.), *Advances in thermal energy storage systems: Methods and applications* (pp. 31–47). Sawston, Cambridge: Woodhead Publishing. https://doi.org/10.1533/9781782420965.1.31

Gossler, M. A., Bayer, P., & Zosseder, K. (2019). Experimental investigation of thermal retardation and local thermal non-equilibrium effects on heat transport in highly permeable, porous aquifers. *Journal of Hydrology*, *578*(August), 12,4097–12,4014. https://doi.org/10.1016/j.jhydrol.2019.124097

Gunn, D. J. (1978). Transfer of heat or mass to particles in fixed and fluidised beds. *International Journal of Heat and Mass Transfer*, *21*(4), 467–476. https://doi.org/10.1016/0017-9310(78)90080-7

Gunn, D. J., & De Souza, J. F. C. (1974). Heat transfer and axial dispersion in packed beds. *Chemical Engineering Science*, *29*(6), 1363–1371. https://doi.org/10.1016/0009-2509(74)80160-0

Hähnlein, S., Bayer, P., Ferguson, G., & Blum, P. (2013). Sustainability and policy for the thermal use of shallow geothermal energy. *Energy Policy*, *59*, 914–925. https://doi.org/10.1016/j.enpol.2013.04.040

Halloran, L. J. S., Rau, G. C., & Andersen, M. S. (2016). Heat as a tracer to quantify processes and properties in the vadose zone: A review. *Earth-Science Reviews*, *159*, 358–373. https://doi.org/10.1016/j.earscirev.2016.06.009

Hamidi, S., Heinze, T., Galvan, B., & Miller, S. (2019). Critical review of the local thermal equilibrium assumption in heterogeneous porous media: Dependence on permeability and porosity contrasts. *Applied Thermal Engineering*, *147*, 962–971. https://doi.org/10.1016/j.applthermaleng.2018.10.130

Heinze, T., & Blöcher, J. R. (2019). A model of local thermal non-equilibrium during infiltration. *Advances in Water Resources*, *132*, 103394. https://doi.org/10.1016/j.advwatres.2019.103394

Heinze, T., & Hamidi, S. (2017). Heat transfer and parameterization in local thermal non-equilibrium for dual porosity continua. *Applied Thermal Engineering*, *114*, 645–652. https://doi.org/10.1016/j.applthermaleng.2016.12.015

Heinze, T., Hamidi, S., & Galvan, B. (2017). A dynamic heat transfer coefficient between fractured rock and flowing fluid. *Geothermics*, *65*, 10–16. https://doi.org/10.1016/j.geothermics.2016.08.007

Herbert, A., Arthur, S., & Chillingworth, G. (2013). Thermal modelling of large scale exploitation of ground source energy in urban aquifers as a resource management tool. *Applied Energy*, *109*, 94–103. https://doi.org/10.1016/j.apenergy.2013.03.005

Huber, M. L., Perkins, R. A., Friend, D. G., Sengers, J. V., Assael, M. J., Metaxa, I. N., et al. (2012). New international formulation for the thermal conductivity of H_2O. *Journal of Physical and Chemical Reference Data*, *41*, 033102. https://doi.org/10.1063/1.4738955

Iooss, B., Da Veiga, S., Janon, A., Pujol, G., Broto, B., Boumhaout, K., et al. (2019). Package "sensitivity" title global sensitivity analysis of model outputs. Retrieved from https://cran.r-project.org/package=sensitivity

Irvine, D. J., Cranswick, R. H., Simmons, C. T., Shanafield, M. A., & Lautz, L. K. (2015). The effect of streambed heterogeneity on groundwater-surface water exchange fluxes inferred from temperature time series. *Water Resources Research*, *51*, 198–212. https://doi.org/10.1002/2014WR015769

Irvine, D. J., Kurylyk, B. L., & Briggs, M. A. (2020). Quantitative guidance for efficient vertical flow measurements at the sediment–water interface using temperature–depth profiles. *Hydrological Processes*, *34*(3), 649–661. https://doi.org/10.1002/hyp.13614

Irvine, D. J., Kurylyk, B. L., Cartwright, I., Bonham, M., Post, V. E. A., Banks, E. W., & Simmons, C. T. (2017). Groundwater flow estimation using temperature-depth profiles in a complex environment and a changing climate. *Science of the Total Environment*, *574*, 272–281. https://doi.org/10.1016/j.scitotenv.2016.08.212

Irvine, D. J., & Lautz, L. K. (2015). High resolution mapping of hyporheic fluxes using streambed temperatures: Recommendations and limitations. *Journal of Hydrology*, *524*, 137–146. https://doi.org/10.1016/j.jhydrol.2015.02.030

Kaviany, M. (1995). *Principles of heat transfer in porous media*, *Mechanical Engineering Series* (Vol. 53). New York, NY: Springer New York. https://doi.org/10.1007/978-1-4612-4254-3

Khashan, S. A., Al-Amiri, A. M., & Pop, I. (2006). Numerical simulation of natural convection heat transfer in a porous cavity heated from below using a non-Darcian and thermal non-equilibrium model. *International Journal of Heat and Mass Transfer*, *49*(5–6), 1039–1049. https://doi.org/10.1016/j.ijheatmasstransfer.2005.09.011

Khashan, S. A., & Al-Nimr, M. A. (2005). Validation of the local thermal equilibrium assumption in forced convection of non-Newtonian fluids through porous channels. *Transport in Porous Media*, *61*(3), 291–305. https://doi.org/10.1007/s11242-004-8305-8

Kim, S. J., & Jang, S. P. (2002). Effects of the Darcy number, the Prandtl number, and the Reynolds number on local thermal non-equilibrium. *International Journal of Heat and Mass Transfer*, *45*(19), 3885–3896. https://doi.org/10.1016/S0017-9310(02)00109-6

Kunii, D., & Smith, J. M. (1961). Heat transfer characteristics of porous rocks: II. Thermal conductivities of unconsolidated particles with flowing fluids. *AICHE Journal*, *7*(1), 29–34. https://doi.org/10.1002/aic.690070109

Kurylyk, B. L., Irvine, D. J., & Bense, V. F. (2019). Theory, tools, and multidisciplinary applications for tracing groundwater fluxes from temperature profiles. *Wiley Interdisciplinary Reviews: Water*, *6*, e1329. https://doi.org/10.1002/wat2.1329

Lee, D. Y., & Vafai, K. (1998). Analytical characterization and conceptual assessment of solid and fluid temperature differentials in porous media. *International Journal of Heat and Mass Transfer*, *42*(3), 423–435. https://doi.org/10.1016/S0017-9310(98)00185-9

Littman, H., Barile, R. G., & Pulsifer, A. H. (1968). Gas-particle heat transfer coefficients in packed beds at low Reynolds numbers. *Industrial and Engineering Chemistry Fundamentals*, *7*(4), 554–561. https://doi.org/10.1021/i160028a005

Minkowycz, W. J., Haji-Sheikh, A., & Vafai, K. (1999). On departure from local thermal equilibrium in porous media due to a rapidly changing heat source: The Sparrow number. *International Journal of Heat and Mass Transfer*, *42*(18), 3373–3385. https://doi.org/10.1016/S0017-9310(99)00043-5

Molina-Giraldo, N., Bayer, P., Blum, P., & Cirpka, O. A. (2011). Propagation of seasonal temperature signals into an aquifer upon bank infiltration. *Ground Water*, *49*(4), 491–502. https://doi.org/10.1111/j.1745-6584.2010.00745.x

Muela Maya, S., García-Gil, A., Garrido Schneider, E., Mejías Moreno, M., Epting, J., Vázquez-Suñé, E., et al. (2018). An upscaling procedure for the optimal implementation of open-loop geothermal energy systems into hydrogeological models. *Journal of Hydrology*, *563*(January), 155–166. https://doi.org/10.1016/j.jhydrol.2018.05.057

Naghash, M., Fathieh, F., Besant, R. W., Evitts, R. W., & Simonson, C. J. (2016). Measurement of convective heat transfer coefficients in a randomly packed bed of silica gel particles using IHTP analysis. *Applied Thermal Engineering*, *106*, 361–370. https://doi.org/10.1016/j.applthermaleng.2016.06.027

Nelson, P. A., & Galloway, T. R. (1975). Particle-to-fluid heat and mass transfer in dense systems of fine particles. *Chemical Engineering Science*, *30*(1), 1–6. https://doi.org/10.1016/0009-2509(75)85109-8

Nie, X., Evitts, R., Besant, R., & Bolster, J. (2011). A new technique to determine convection coefficients with flow through particle beds. *Journal of Heat Transfer*, *133*(4), 1–8. https://doi.org/10.1115/1.4002945

Nield, D. A., & Bejan, A. (2017). *Convection in porous media* (5th ed., Vol. 3). Cham: Springer International Publishing. https://doi.org/10.1007/978-3-319-49562-0

Park, B. H., Bae, G. O., & Lee, K. K. (2015). Importance of thermal dispersivity in designing groundwater heat pump (GWHP) system: Field and numerical study. *Renewable Energy*, *83*, 270–279. https://doi.org/10.1016/j.renene.2015.04.036

Park, B. H., Lee, B. H., & Lee, K. K. (2018). Experimental investigation of the thermal dispersion coefficient under forced groundwater flow for designing an optimal groundwater heat pump (GWHP) system. *Journal of Hydrology*, *562*(May), 385–396. https://doi.org/10.1016/j.jhydrol.2018.05.023

Peterson, R. A., & Cavanaugh, J. E. (2019). Ordered quantile normalization: A semiparametric transformation built for the cross-validation era. *Journal of Applied Statistics*, *47*(13–15), 2312–2327. https://doi.org/10.1080/02664763.2019.1630372

Pophillat, W., Bayer, P., Teyssier, E., Blum, P., & Attard, G. (2020). Impact of groundwater heat pump systems on subsurface temperature under variable advection, conduction and dispersion. *Geothermics*, *83*(February) 2019, 101721. https://doi.org/10.1016/j.geothermics.2019.101721

Quintard, M., Kaviany, M., & Whitaker, S. (1997). Two-medium treatment of heat transfer in porous media: Numerical results for effective properties. *Advances in Water Resources*, *20*(2-3 SPEC. ISS), 77–94. https://doi.org/10.1016/s0309-1708(96)00024-3

Ranz, W., & Marshall, W. R. (1952). Evaporation from drops 1. *Chemical Engineering Progress*, *48*(3), 173–180.

Rau, G. C., Andersen, M. S., & Acworth, R. I. (2012a). Experimental investigation of the thermal dispersivity term and its significance in the heat transport equation for flow in sediments. *Water Resources Research*, *48*, W03511. https://doi.org/10.1029/2011WR011038

Rau, G. C., Andersen, M. S., & Acworth, R. I. (2012b). Experimental investigation of the thermal time-series method for surface water-groundwater interactions. *Water Resources Research*, *48*, W03530. https://doi.org/10.1029/2011WR011560

Rau, G. C., Andersen, M. S., McCallum, A. M., & Acworth, R. I. (2010). Analytical methods that use natural heat as a tracer to quantify surface water-groundwater exchange, evaluated using field temperature records. *Hydrogeology Journal*, *18*(5), 1093–1110. https://doi.org/10.1007/s10040-010-0586-0

Rau, G. C., Andersen, M. S., McCallum, A. M., Roshan, H., & Acworth, R. I. (2014). Heat as a tracer to quantify water flow in near-surface sediments. *Earth-Science Reviews*, *129*, 40–58. https://doi.org/10.1016/j.earscirev.2013.10.015

Rau, G. C., Halloran, L. J. S., Cuthbert, M. O., Andersen, M. S., Acworth, R. I., & Tellam, J. H. (2017). Characterising the dynamics of surface water-groundwater interactions in intermittent and ephemeral streams using streambed thermal signatures. *Advances in Water Resources*, *107*, 354–369. https://doi.org/10.1016/j.advwatres.2017.07.005

Rees, D. A. S., Bassom, A. P., & Siddheshwar, P. G. (2008). Local thermal non-equilibrium effects arising from the injection of a hot fluid into a porous medium. *Journal of Fluid Mechanics*, *594*, 379–398. https://doi.org/10.1017/S0022112007008890

Rosenberry, D. O., Lewandowski, J., Meinikmann, K., & Nützmann, G. (2015). Groundwater - the disregarded component in lake water and nutrient budgets. Part 1: Effects of groundwater on hydrology. *Hydrological Processes*, *29*(13), 2895–2921. https://doi.org/10.1002/hyp.10403

Roshan, H., Cuthbert, M. O., Andersen, M. S., & Acworth, R. I. (2014). Local thermal non-equilibrium in sediments: Implications for temperature dynamics and the use of heat as a tracer. *Advances in Water Resources*, *73*, 176–184. https://doi.org/10.1016/j.advwatres.2014.08.002

Saltelli, A. (2002). Making best use of model evaluations to compute sensitivity indices. *Computer Physics Communications*, *145*(2), 280, https://doi.org/10.1016/S0010-4655(02)00280-1–297.
Schwarz, G. (1978). Estimating the dimension of a model. *The Annals of Statistics*, *6*(2), 461–464. https://doi.org/10.1214/aos/1176344136
Seibert, S., Prommer, H., Siade, A., Harris, B., Trefry, M., & Martin, M. (2014). Heat and mass transport during a groundwater replenishment trial in a highly heterogeneous aquifer. *Water Resources Research*, *50*, 9463–9483. https://doi.org/10.1002/2013WR015219
Shaik, A. R., Rahman, S. S., Tran, N. H., & Tran, T. (2011). Numerical simulation of fluid-rock coupling heat transfer in naturally fractured geothermal system. *Applied Thermal Engineering*, *31*(10), 1600–1606. https://doi.org/10.1016/j.applthermaleng.2011.01.038
Shent, J., Kaguei, S., & Wakao, N. (1981). Measurements of particle-to-gas heat transfer coefficients from one-shot thermal responses in packed beds. *Chemical Engineering Science*, *36*(8), 1283–1286. https://doi.org/10.1016/0009-2509(81)80162-5
Singhal, A., Cloete, S., Radl, S., Quinta-Ferreira, R., & Amini, S. (2017a). Heat transfer to a gas from densely packed beds of cylindrical particles. *Chemical Engineering Science*, *172*, 1–12. https://doi.org/10.1016/j.ces.2017.06.003
Singhal, A., Cloete, S., Radl, S., Quinta-Ferreira, R., & Amini, S. (2017b). Heat transfer to a gas from densely packed beds of monodisperse spherical particles. *Chemical Engineering Science*, *172*, 1–12. https://doi.org/10.1016/j.cej.2016.12.12
Skeel, R. D., & Berzins, M. (1990). A method for the spatial discretization of parabolic equations in one space variable. *SIAM Journal on Scientific and Statistical Computing*, *11*(1), 1–32. https://doi.org/10.1137/0911001
Somogyvári, M., & Bayer, P. (2017). Field validation of thermal tracer tomography for reconstruction of aquifer heterogeneity. *Water Resources Research*, *53*, 5070–5084. https://doi.org/10.1002/2017WR020543
Somogyvári, M., Bayer, P., & Brauchler, R. (2016). Travel-time-based thermal tracer tomography. *Hydrology and Earth System Sciences*, *20*(5), 1885–1901. https://doi.org/10.5194/hess-20-1885-2016
Sözen, M., & Vafai, K. (1990). Analysis of the non-thermal equilibrium condensing flow of a gas through a packed bed. *International Journal of Heat and Mass Transfer*, *33*(6), 1247–1261. https://doi.org/10.1016/0017-9310(90)90255-S
Sun, B., Tenneti, S., & Subramaniam, S. (2015). Modeling average gas-solid heat transfer using particle-resolved direct numerical simulation. *International Journal of Heat and Mass Transfer*, *86*, 898–913. https://doi.org/10.1016/j.ijheatmasstransfer.2015.03.046
Tavassoli, H., Kriebitzsch, S. H. L., van der Hoef, M. A., Peters, E. A. J. F., & Kuipers, J. A. M. (2013). Direct numerical simulation of particulate flow with heat transfer. *International Journal of Multiphase Flow*, *57*, 29–37. https://doi.org/10.1016/j.ijmultiphaseflow.2013.06.009
Tavassoli, H., Peters, E. A. J. F., & Kuipers, J. A. M. (2015). Direct numerical simulation of fluid-particle heat transfer in fixed random arrays of non-spherical particles. *Chemical Engineering Science*, *129*, 42–48. https://doi.org/10.1016/j.ces.2015.02.024
Urumović, K., & Urumović, K. (2014). The effective porosity and grain size relations in permeability functions. *Hydrology and Earth System Sciences Discussions*, *11*(6), 6675–6714. https://doi.org/10.5194/hessd-11-6675-2014
van Genuchten, M. T., & Alves, W. J. (1982). *Analytical solutions of the one-dimensional convective-dispersive solute transport equation*, *Technical Bulletin* (Vol. 1661). Washington: United States Department of Agriculture. https://doi.org/10.1016/0378-3774(84)90020-9
Wakao, N., & Kaguei, S. (1982). *Heat and mass transfer in packed beds*. New York: Gordon and Breach Science Publishers.
Wakao, N., Kaguei, S., & Funazkri, T. (1979). Effect of fluid dispersion coefficients on particle-to-fluid heat transfer coefficients in packed beds. Correlation of Nusselt numbers. *Chemical Engineering Science*, *34*(3), 325–336. https://doi.org/10.1016/0009-2509(79)85064-2
Whitaker, S. (1991). Improved constraints for the principle of local thermal equilibrium. *Industrial and Engineering Chemistry Research*, *30*(5), 983–997. https://doi.org/10.1021/ie00053a022
Zanoni, M. A. B., Torero, J. L., & Gerhard, J. I. (2017). Determination of the interfacial heat transfer coefficient between forced air and sand at Reynold's numbers relevant to smouldering combustion. *International Journal of Heat and Mass Transfer*, *114*, 90–104. https://doi.org/10.1016/j.ijheatmasstransfer.2017.06.020
Zhang, X., Liu, W., & Liu, Z. (2009). Criterion for local thermal equilibrium in forced convection flow through porous media. *Journal of Porous Media*, *12*(11), 1103–1111. https://doi.org/10.1615/JPorMedia.v12.i11.60
Zhu, L. T., Liu, Y. X., & Luo, Z. H. (2019). An enhanced correlation for gas-particle heat and mass transfer in packed and fluidized bed reactors. *Chemical Engineering Journal*, *374*, 531–544. https://doi.org/10.1016/j.cej.2019.05.194